

Substituent Effects on Configurational Stabilities at Tetrahedral Boron Atoms in Intramolecular Borane–Amine Complexes: Structures, Enantiomeric Resolution, and Rates of Enantiomerization of [2-(Dimethylaminomethyl)phenyl]phenylboranes[#]

Shinji Toyota,* Fumiko Ito, Naoya Nitta, and Tomohiro Hakamata

Department of Chemistry, Faculty of Science, Okayama University of Science, 1-1 Ridaicho, Okayama 700-0005

Received June 1, 2004; E-mail: stoyo@chem.ous.ac.jp

The structures and stereochemistries of the five borane–amine complexes, (*N*–*B*)-{2-(Me_2NCH_2)C_6H_4}BPhX (X = Cl, F, Me, –$OCOCF_3$, and –$OCOC_2F_5$), were studied by some spectroscopic methods. The Cl complex prepared by the standard method was converted to each of the other complexes by the treatment with an appropriate reagent (MeLi or AgX). The enantiomers of the two perfluoroacyloxy complexes were resolved by chiral HPLC as a novel intramolecular borane–amine complex with a chiral center at the tetrahedral boron atom, and their chiroptical properties were investigated by optical rotations and CD spectra. The classical kinetics or the saturation transfer measurements revealed that the barriers to enantiomerization via the dissociation of the B–N coordination bond were enhanced from 94 to 116 kJ mol^{-1} in the following order of X: F < Me < –$OCOCF_3$ ≈ Cl < –$OCOC_2F_5$. The substituent effects on the configurational stability, which is closely related to the Lewis acidity of boron atoms, are discussed on the basis of the X-ray structures of the three complexes.

We have studied the structures and the mechanism of dynamic behavior of intramolecular borane–amine complexes **1**–**3** with a 2-(dimethylaminomethyl)phenyl (DMP) group as a bidentate *C*,*N* ligand (Chart 1).[2–6] The spectroscopic analyses revealed that the strength of the intramolecular B–N coordination bond was influenced by various factors, such as substituents and solvents. These results are valuable to estimate the Lewis acidity of boron atoms and the Lewis basicity of nitrogen atoms. Moreover, a series of structural data led us to propose the "tetrahedral character" for the structural correlation between the geometry of boron atoms and their Lewis acidity.[7] In most of these complexes, the boron atoms are configurationally liable in solution because of facile isomerization via the B–N bond dissociation, even though the boron atom is bonded to four different ligands including a DMP ligand.

Chiral compounds with a stereogenic center at the tetrahedral boron atom are intriguing targets in the stereochemical studies in relation to the chemistry of tetrahedral carbons.[8] Such boron compounds have been investigated from various aspects,[9] leading to several examples of isolable enantiopure borates and coordinated boranes.[10–16] In most cases, the configuration at a boron atom is derived by other chiral elements in an identical molecule with enantiopure moieties such as amino acids and terpenes, some of which have been successfully utilized in the organic synthesis.[11,12] Recently, enantiopure compounds with a chiral boron center as the sole stereogenic center have attracted interest, and two types of complexes with phosphine and amine ligands (**4** and **5**) were reported.[17,18] These complexes carry one hydrogen ligand on the boron atom, namely they are isoelectronic to secondary carbons, and they provide direct evidence of the S_N2 reaction at the boron atom with inversion. These results tempted us to explore chiral borane complexes by using the DMP ligand. Accordingly, we found that the title intramolecular borane–amine complexes (**6**) were suitable for our purpose; here the boron atom carried a phenyl group[19] and a ligand X in addition to the *C*,*N*-bidentate ligand (Chart 2). In the structural system,

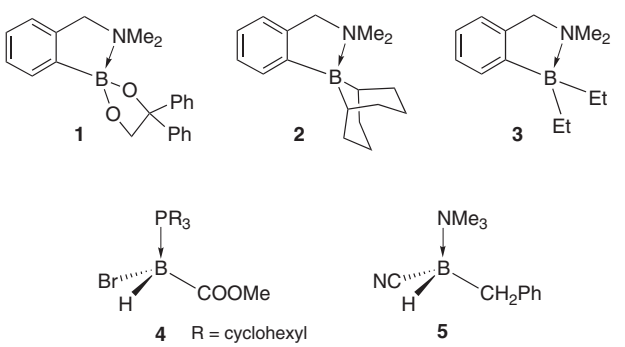

Chart 1.

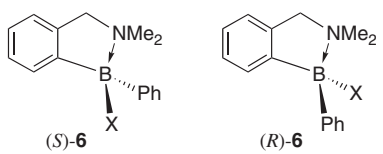

a X = Cl
b X = Me
c X = F
d X = $OCOCF_3$
e X = $OCOC_2F_5$
(*R* and *S* are vise verse for **6b**.)

Chart 2.

Published on the web November 11, 2004; DOI 10.1246/bcsj.77.2081

we can introduce various substituents at the boron atom, facilitating the tuning of the structural and dynamic properties. Fortunately, we could successfully resolve the enantiomers as novel optically active intramolecular borane–amine complexes when perfluoroacyloxy groups were introduced as X. We herein report the structure and configurational stability of a series of (DMP)phenylboranes. The substituent effects on the Lewis acidity of boron atoms are discussed on the basis of the kinetic data and the X-ray structures.

Results and Discussion

Synthesis and ^{11}B NMR. Complexes **6** were prepared according to Scheme 1. (DMP)lithium was prepared by *o*-lithiation of *N*,*N*-dimethylbenzylamine **7** with butyllithium in an ordinary manner. This reagent was treated with dichlorophenylborane to afford the corresponding chlorophenylborane **6a** in 66% yield. The reaction of **6a** with methyllithium or a silver reagent gave the corresponding boranes **6b–e** in good yields. These compounds are colorless crystals that are stable under ambient condition.

^{11}B NMR spectra of **6** were measured in chloroform-*d*. The chemical shift data are compiled in Table 1 together with those of coordination free boranes as references.[20,21] The signals of **6** were observed as broad bands in the range of δ 6–13. These chemical shifts are shifted upfield by 35–65 ppm compared with the reference compounds; such shifts are typical of tetracoordinated boron atoms.[22]

Table 1. ^{11}B NMR Chemical Shifts of **6** and Coordination-Free Reference Compounds[a)]

Compound (X)	δ/ppm	δ/ppm (Compound)[b)]
6a (Cl)	10.8	61.0 (Ph_2BCl)
6b (Me)	6.8	70.6 (Ph_2BMe)
6c (F)	12.6	47.4 (Ph_2BF)
6d ($OCOCF_3$)	11.3	45.1 (Ph_2BOEt), 47.8 (Et_2BOAc)[c)]
6e ($OCOC_2F_5$)	8.8	

a) Reference $BF_3 \cdot OEt_2$ at δ 0. Solvent $CDCl_3$. b) Refs. 20 and 21. c) ^{11}B NMR data of acyloxydiphenylboranes (Ph_2BOCOR) are not available.

X-ray Analysis. Molecular structures of **6a**, **6b**, and **6e** were analyzed by X-ray crystallography. ORTEP drawings are shown in Fig. 1. Selected structural parameters around the boron atoms are listed in Table 2.

In each complex, the boron atom is internally coordinated by the amino-nitrogen atom to take a tetrahedral geometry. The B–N bond distances are 1.67 Å in **6a** and **6e**, and that in **6b** is longer by ca. 0.04 Å than the others. The database

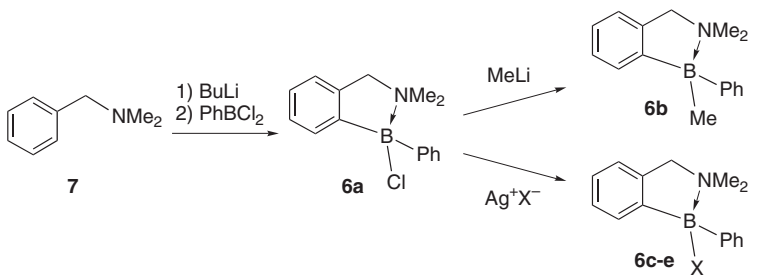

Scheme 1. Synthesis of complexes **6**.

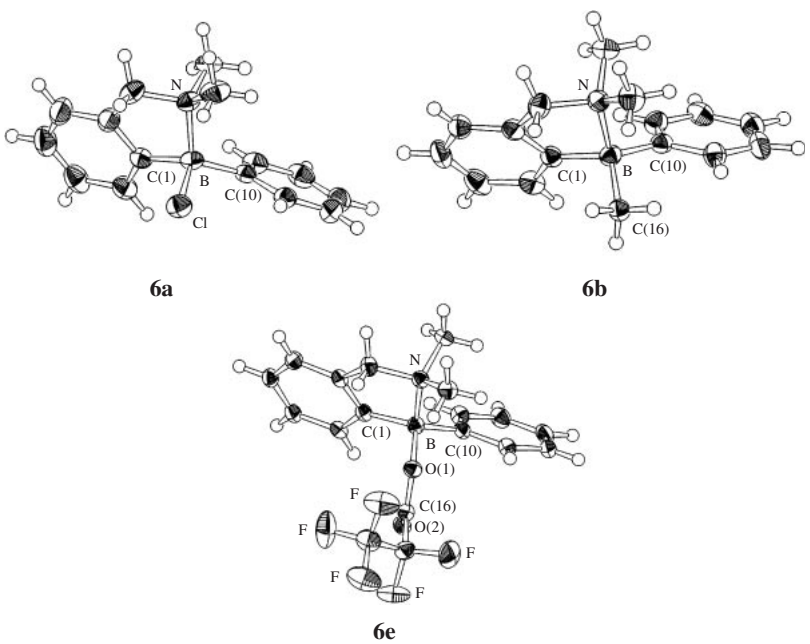

Fig. 1. ORTEP drawings of **6a**, **6b**, and **6e**.

Table 2. Selected Structural Parameters in X-ray Structures of **6**[a)]

	6a	**6b**(A)[b)]	**6b**(B)[b)]	**6e**
Bond length/Å				
B–N	1.667(2)	1.707(4)	1.704(4)	1.668(4)
B–C(1)	1.599(2)	1.628(4)	1.605(4)	1.600(4)
B–C(10)	1.597(3)	1.618(4)	1.635(4)	1.604(4)
B–X′[c)]	1.920(2)	1.666(4)	1.656(4)	1.535(3)
Bond angle/degree				
X′–B–C(1)	107.5(1)	110.0(2)	110.4(2)	110.4(2)
X′–B–C(10)	109.7(1)	113.0(2)	112.6(2)	111.8(2)
C(1)–B–C(10)	121.6(1)	117.1(2)	117.2(2)	120.2(2)
THC/%[d)]	67	63	63	56

a) Standard deviations in parentheses. b) Data for two independent molecules A and B in an asymmetric unit. Figure 1 shows the structure of A. c) X′ stands for the atom directly attached to the boron atom in group X. d) Tetrahedral character at the boron atom. Ref. 7.

analysis revealed that the distances of B–N coordination bonds were in the range of 1.67–1.76 Å in ordinary borane–amine complexes.[23] The observed distances of **6** are within the range, suggesting that the coordinated form suffers from little strain by the formation of the five-membered ring. The tetrahedral character (THC) was calculated from bond angles at the boron atom: this structural parameter was proposed for the correlation between the structure and the strength of Lewis acidity of boron compounds.[7,24] The values increase from 56 to 67% in the order of **6e** < **6b** < **6a**. Generally, the THC value tends to be large when the boron atom is bonded to electronegative atoms. The large value of **6a** is explained by the substitution of an electronegative chlorine atom; the value is comparable to that of a similar intramolecular chloroborane–amine complex, (*N–B*)-[2-(Me_2N)$C_6H_4CH_2$]BClPh (B–N 1.685(4) Å and THC 65%).[25] The THC value of **6e** is smaller than those of other intramolecular diphenylborinate–amine adducts (74–80%).[7,24] The correlation of these structural parameters with the rates of the B–N bond dissociation will be discussed later.

In **6e**, the torsion angles of N–B–O(1)–C(16) and B–O(1)–C(16)–O(2) are 176.6(2) and 0.0(4)°, respectively. Namely, the carbonyl carbon is *anti* relative to the amine ligand along the B–O(1) bond, and the carbonyl oxygen is perfectly *syn* relative to the boron atom along the O(1)–C(16) bond.

Enantiomeric Resolution and Chiroptical Properties. Resolution of the enantiomers of **6** was attempted by chiral HPLC under various conditions. The chloride **6a** completely decomposed during the separation in an eluent system of hexane–alcohol, even though its barrier to racemization was high enough for the resolution at room temperature, as is mentioned later. **6b** and **6c** were eluted as a single peak under all conditions because of facile racemization or poor resolution.

In contrast, the use of a Daicel Chiralpak AD column gave good results for the acyloxy compounds. The enantiomers of **6d** were partially resolved at the retention times of 16.2 and 16.6 min (separation coefficient $\alpha = 1.29$) with hexane–2-propanol 1:1 as eluent. However, further separation in a large scale was difficult due to poor solubility and partial decomposition. The partially resolved samples are dextro- and levorotatory in the order of elution. **6e** was effectively resolved without these problems. The enantiomers were eluted at 21.0 and 27.7 min with the base-line separation ($\alpha = 1.49$) with hexane–2-propanol 50:1 as eluent. The specific rotations of the first and second fractions were $[\alpha]_D^{22}$ +180 and −180, respectively, in acetone. While the racemization of **6e** was negligibly slow in solutions at room temperature, it occurred rapidly at higher temperatures.

CD spectra of enantiomers of **6e** were measured in hexane (Fig. 2(a)). The (+)-isomer afforded a weak trough at 224 nm ($\Delta\varepsilon$ −4.3) with a positive broad shoulder extending to the shorter wavelength region; these features are mainly attributed to π–π^* transitions of benzene chromophors. The spectrum of the (−)-isomer was practically the mirror image of that of the (+)-isomer. The decrease in the CD intensity was observed as an enantiopure sample underwent racemization by heat: for example, the course of racemization of (−)-**6e** is inserted in Fig. 2(a). The partially resolved samples of **6d** are also CD active, and the easily eluted (+)-isomer gave a similar CD curve to that of (+)-**6e** (Fig. 2(b)). This chiroptical similarity suggests that the (+)-isomers (or (−)-isomers) of **6d** and **6e** must have the same stereochemistry, although their absolute configuration cannot be assigned from the available data. Theoretical studies or X-ray analysis will solve the question.

The above data are typical of enantiomers; their chiroptical activity depends only on the chiral center at the boron atoms. As for borane–Lewis base adducts, only two types of such optically active organoboron compounds, **4** and **5**, are known, in which the tetrahedral boron atom is bonded to one hydrogen atom and three nonhydrogen ligands.[16,17] Accordingly, **6e** is the first example of an enantiopure borane complex with four nonhydrogen ligands, to the best of our knowledge, the central boron atom being isoelectronic to a tertiary carbon atom.

Barrier to Enantiomerization. The ^{1}H NMR spectra of **6** afforded two singlets due to the *N*-Me groups and an AB quartet due to the benzylic methylene protons at room temperature and even at 130 °C in 1,1,2,2-tetrachloroethane-d_2 (TCE). This signal pattern is consistent with the coordinated form, where the methylene protons and the *N*-Me groups are diastereotopic because of the chiral boron center. The absence of lineshape changes suggests that the dynamic process takes place much more slowly than the NMR time scale at the temperature, its barrier being higher than 90 kJ mol^{-1}. Because the complex began to decompose at higher temperatures, we were not able to adopt the lineshape analysis for the kinetic measurement.

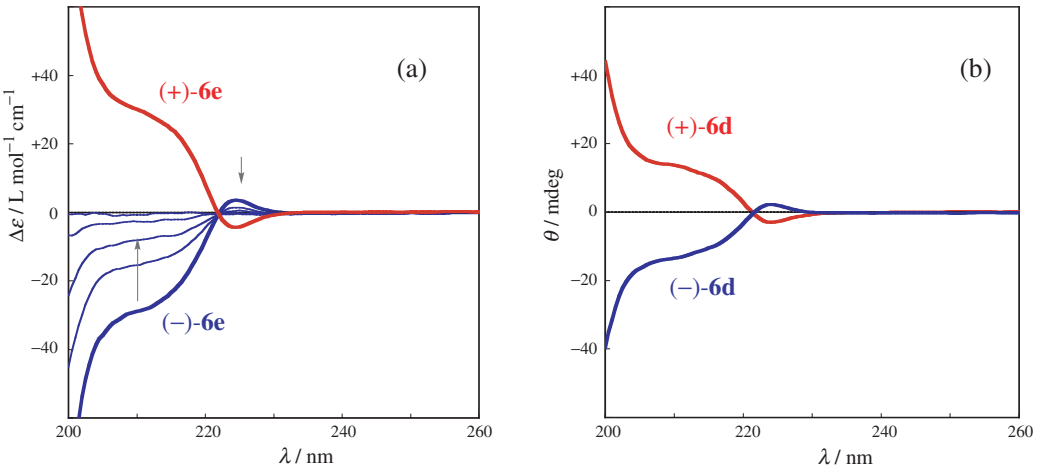

Fig. 2. CD spectra of **6d** and **6e** in hexane. (a) Enantiopure samples of (+)- and (−)-**6e**. Spectral changes during the racemization of (−)-**6e** upon heating for 0, 70, 300, 600, and 1080 min at 69 °C are indicated by arrows. (b) Enantioenriched samples of (+)- and (−)-**6d**.

Table 3. Kinetic Data of Enantiomerization in Complexes **6** and Related Compounds

Compound	Method[a)]	Solvent	t/°C	k/s^{-1}	$\Delta G_t^{\neq}$/kJ mol^{-1}
6a	ST	$C_2D_2Cl_4$[b)]	135	4.4×10^{-2}	112
6b	ST	$C_2D_2Cl_4$	140	0.75	103
6c	ST	$C_2D_2Cl_4$	120	2.6	94
6c	ST	$C_6D_5NO_2$	120	2.1	95
6d	ST	$C_2D_2Cl_4$	135	0.12	108
6d	CK	heptane	73	9.6×10^{-5}	112
6e	CK	heptane	83	6.4×10^{-5}	116
2[c)]	TLA	$C_6D_5CD_3$	120	1.2×10^{3}	74
3[d)]	TLA	$C_2D_2Cl_4$	120	15	88

a) ST: saturation transfer. CK: classical kinetics. TLA: total lineshape analysis. b) 1,1,2,2-Tetrachloroethane-d_2 (TCE). c) Ref. 4. d) Ref. 5.

Thus, we carried out the saturation transfer (ST) experiments;[26,27] these allowed us to follow slower kinetic processes. Actually, when one of the Me proton signals of **6c** was irradiated at 120 °C in TCE, the intensity of the other Me proton signal became about a half of the original signal. A quantitative analysis afforded the rate of site exchange between the two Me groups at 2.6 s^{-1}, corresponding to 94 kJ mol^{-1} in free energy of activation. The magnetization transfers were small for **6a**, **6b**, and **6d**, and negligible for **6e** at 130–140 °C, the highest limit of temperature for measurements without decomposition. The kinetic data are listed in Table 3.

The rates of enantiomerization were determined by the classical kinetics measurement for **6d** and **6e**. When an enantiopure sample of **6e** was heated at 83 °C in heptane, the racemization was almost completed in 4 h. The course of racemization was monitored by chiral HPLC, and the kinetic analysis afforded the rate constant (6.4×10^{-5} s^{-1}) and the free energy of activation for enantiomerization (116 kJ mol^{-1}). The rate constants were also determined at five different temperatures in the range of 73–93 °C to give the following kinetic data: $\Delta H^{\neq}$ 146 ± 10 kJ mol^{-1} and $\Delta S^{\neq}$ 84 ± 29 J mol^{-1} K^{-1}. The rate of **6d** was determined with a partially resolved sample in heptane at 73 °C. The relative change in the enantiomeric excess was monitored by the CD spectra. Thus obtained barrier height (112 kJ mol^{-1}) is comparable to that determined by the ST method.

Mechanism of Racemization. Before one compares the data in Table 3, it is instructive to understand the kinetic relationship between the rate constants of possible dynamic processes. There are three elementary processes: the dissociation of the B–N bond (rate constant: k_{dis}), the rotation about the B–C(1) bond (k_{rot}), and the inversion at the nitrogen atom (k_{inv}). These rate constants determine those of experimentally observable processes, the enantiomerization (k_{ena})[28] and the site exchange between the two *N*-Me signals (k_{Me}). A possible mechanism of enantiomerization and the related processes is shown in Scheme 2.

In general, the nitrogen inversion takes place much faster than the NMR time scale in acyclic amines: for example the barrier to inversion is 45 kJ mol^{-1} for dialkylbenzylamines.[29] As for the B–C bond rotation, the barriers are not so high in triarylboranes and alkoxydiarylboranes (45–55 kJ mol^{-1}) even though aryl groups are sterically bulky such as the mesityl group.[30] These experimental facts strongly support that both the N inversion and the B–C rotation take place rapidly after the dissociation of the B–N bond under the conditions of the kinetic measurements in **6**, namely $k_{dis} \ll k_{inv}$, k_{rot}. Under the situation, once the coordination bond dissociates, the N

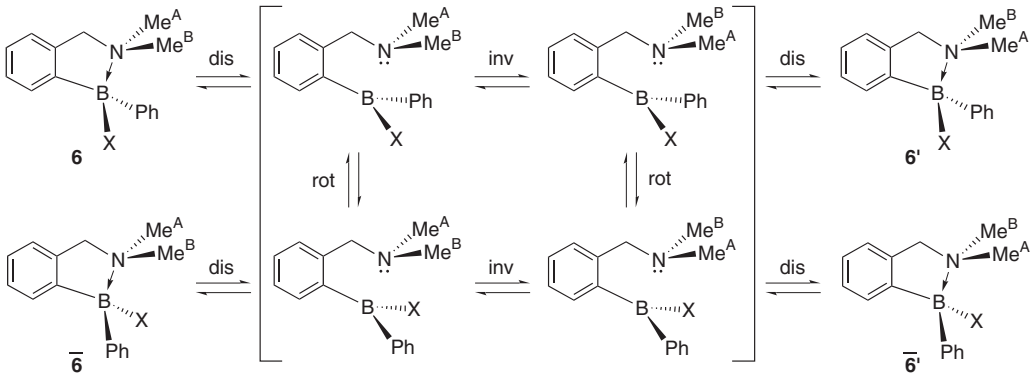

Scheme 2. Circuit of dynamic processes in **6**. dis: dissociation of B–N bond. inv: N inversion. rot: C–B bond rotation. Bars and primes refer to the relations of enantiomers and topomers, respectively.

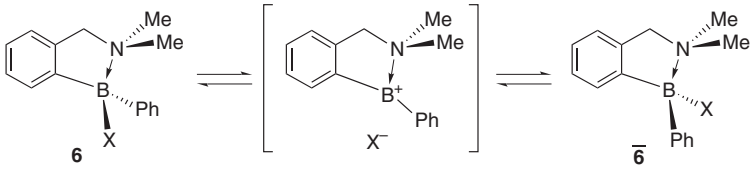

Scheme 3. Enantiomerization via ionic dissociation in **6**.

atom recombines with the trigonal B atom from two prochiral faces randomly as seen in the S_N1 reaction at tertiary carbon atoms ($k_{ena} = k_{dis}/2$). The site exchange between the *N*-Me groups is also accompanied by the B–N dissociation. The facile N inversion in the dissociated form scrambles the magnetic sites of the two Me groups regardless of enantiomerization. Namely, a Me group comes back to the same site and the other with the same probabilities via the dissociation ($k_{Me} = k_{dis}/2$). We can rationalize the kinetic relationship of $k_{ena} = k_{Me} = k_{dis}/2$ from the above discussion. It is a piece of supporting evidence of this mechanism that the free energies of activation for enantiomerization and the Me exchange determined by the independent methods are nearly equal, namely $k_{ena} \approx k_{Me}$ at the same temperature, for **6d**.

Another possible pathway of racemization involves the dissociation of the B–X bond instead of the B–N bond in **6**. The dissociation energies of the B–O, B–halogen, and B–C bonds are so large that the homolytic dissociation is unlikely under the conditions of the kinetic measurements.[31] The ionic dissociation mechanism shown in Scheme 3 is also eliminated for the following reasons. Firstly, the rate of enantiomerization was not affected so much for **6c** even though nitrobenzene-d_5 was used as solvent (Table 3). If the B–F bond were to dissociate, the strongly polar solvent should considerably accelerate the dissociation. Secondly, the entropy of activation ($\Delta S^{\neq}$) of enantiomerization of **6e** is large and positive; this tendency is characteristic of the dissociation of the B–N coordination bond rather than that of the B–O bond.[32] While the former process decreases the ionic character in the transition state relative to the initial state, the situation should be vise versa in the latter process, to give a negative $\Delta S^{\neq}$ value.

The above discussion ensures that the dissociation of the B–N bond is rate-determining in the overall enantiomerization process and that the kinetic data determined by the ST method are equivalent to those of enantiomerization in the intramolecular borane–amine system.

Substituent Effects on Lewis Acidity. Because the DMP moiety is common in all complexes **6**, the barrier to enantiomerization is closely related to the Lewis acidity of boron atoms: the higher the barrier, the more acidic. According to this kinetic measure, the acidity is enhanced in the order of **6c** (F) < **6b** (Me) < **6d** ($OCOCF_3$) ≈ **6a** (Cl) < **6e** ($OCOC_2F_5$). This order is not always consistent with the general trend in BY_3 type boranes: $B(OR)_3 < BR_3 < BAr_3 < BF_3 < BCl_3$ (R = alkyl, Ar = aryl).[31,33] It is known that the Lewis acidity of borane derivatives is influenced by various factors such as electronic and steric effects. In the case of **6**, the effects at the coordinated and dissociated forms determine the overall Lewis acidity. The weak Lewis acidity of **6c** may be explained by the fact that the stabilization of the dissociated form (transition state) by π type B–F interactions works more effectively in the system of **6** than in simple boranes. Relatively little is known about the influences of acyloxy groups on the Lewis acidity of attaching boron atoms. The above data unambiguously show that the effect of a $-OCOCF_3$ group is comparable to that of a Cl group, and a $-OCOC_2F_5$ group further enhances the acidity. In general, oxygen substituents on B atoms weaken the Lewis acidity by the resonance effect: for example, weakly acidic boronic acids or alkyl borates. This effect is overwhelmed by a strongly electron-withdrawing moiety in the perfluoroacyloxy compounds. The difference in barriers to enantiomerization between **6d** and **6e** is attributed to the inductive effect of extra fluorine atoms in the latter, which slightly increases the Lewis acidity of the boron atom. This finding is consistent with the pK_a values of trifluoroacetic acid (0.52) and pentafluoropropionic acid (−0.41).[34] The use of a $-OCOC_2F_5$ group not only enhances the barrier to enantiomerization but also increases the chemical stability and the solubility. These advantages greatly facilitate the enantiomeric resolution and the handling of enantiopure samples of **6e**.

The kinetic and structural data of **6** as well as of **1** ($\Delta G^{\neq}$ 39 kJ mol^{-1} at 120 °C, B–N 1.754 Å, THC 51%) and of **2** ($\Delta G^{\neq}$ 74 kJ mol^{-1} at 120 °C, B–N 1.746 Å, THC 72%) indicate that the barriers to enantiomerization are enhanced as the B–N bonds become short. On the contrary, the barrier heights are not always correlated with the THC in these compounds. The THC value of **6e** is smaller than those of **6a**, **6b**, and **2** regardless of the tight coordination bond. This finding means that perfluoroacyloxy groups tend to enhance the Lewis acidity of boron atoms with a small structural change from trigonal to tetrahedral geometry. In the series of trialkyl(aryl)borane–amine complexes, the barriers to dissociation are enhanced in the order of **2** < **3** < **6b**. The strong acidity of **6b** is attributed to the inductive effect of a phenyl group, which is more electronegative than alkyl groups. It is notable that the THC value of **6b** is smaller than that of **2** (72%) contrary to the tight coordination in the former. These structural and kinetic features of **2** are considerably influenced by the steric effect of the bulky 9-BBN moiety, which destabilizes the coordinated form by the F-strain. The above results show that the THC values are influenced not only by the strength of coordination bond but also by various factors such as the electronegativity of attached atoms and the steric effect.

In summary, a series of (DMP)phenylboranes with a tetrahedral chiral boron center were synthesized to probe the substituent effects on the ease of enantiomerization or the Lewis acidity. The stable enantiopure borane–amine complexes, especially the –OCOC$_2$F$_5$ complex, lead to a novel design of chiral tetrahedral boranes as enantioselective reagents in the organic chemistry. The kinetic analysis of enantiomerization process reveals the mechanism of the configurational liability at the boron atom via the dissociation of B–N bond, which is isoelectronically related to the S_N1 reaction at a tertiary carbon atom.

Experimental

General. Melting points are uncorrected. ^{1}H and ^{13}C NMR spectra were measured on a Varian Gemini-300 spectrometer at 300 and 75 MHz, respectively. ^{11}B and ^{19}F NMR spectra were measured on a JEOL Lambda-300 spectrometer at 96 and 282 MHz, respectively. Optical rotations were measured on a JASCO DIP-1000 digital polarimeter with a 3.5 mm $\phi \times$ 100 mm cell. CD spectra were measured on a JASCO J-810 polarimeter with a 1 mm cell.

Chloro[2-(dimethylaminomethyl)phenyl]phenylborane (6a). To a solution of 2.0 mL (13 mmol) of *N*,*N*-dimethylbenzylamine in 20 mL of dry hexane was added 9.2 mL (14 mmol) of a 1.0 mol L^{-1} butyllithium solution in hexane at −78 °C under argon atmosphere. The reaction mixture was allowed to warm up to room temperature, and then stirred for 24 h under reflux. The white suspension thus prepared was slowly transferred with a cannula into a solution of dichlorophenylborane (1.8 mL or 13 mmol) in 20 mL of dry hexane in an ice bath. After the mixture was stirred at room temperature for 4 h, the volatile materials were removed by evaporation. The residue was extracted with dichloromethane. The organic solution was washed with aqueous sodium hydrogencarbonate, dried over anhydrous magnesium sulfate, and then evaporated. The crude product was purified by recrystallization from hexane–dichloromethane to give 2.28 g (66%) of the pure material as colorless needles; mp 154–156 °C; ^{1}H NMR ($CDCl_3$) δ 2.26 (3H, s), 2.95 (3H, s), 3.94 and 4.54 (2H, ABq, J = 13.0 Hz), 7.20 (1H, d, J = 7.3 Hz), 7.26–7.36 (5H, m), 7.57 (1H, d, J = 6.3 Hz), 7.66 (2H, dd, J = 7.5, 1.7 Hz); ^{13}C NMR ($CDCl_3$) δ 46.4, 48.5, 67.8, 122.3, 127.2, 127.3, 127.4, 127.7, 130.8, 134.1, 138.8, 141.4 (br), 148.2 (br); ^{11}B NMR ($CDCl_3$) δ 10.8 (half-band width 151 Hz); Anal. Found: C, 69.67; H, 6.77; N, 5.33%. Calcd for $C_{15}H_{17}BClN$: C, 69.95; H, 6.65; N, 5.44%.

[2-(Dimethylaminomethyl)phenyl]methylphenylborane (6b). To a solution of 370 mg (1.42 mmol) of **6a** in 10 mL of toluene was added 1.3 mL (1.4 mmol) of a 1.1 mol L^{-1} methyllithium solution in hexane under argon atmosphere. After the mixture was stirred for 15 h at room temperature, the solvent was evaporated. The residue was extracted with dichloromethane, and insoluble materials were removed by filtration. The crude product was purified by recrystallization from hexane–dichloromethane to give 224 mg (66%) of the desired product as colorless crystals; mp 130–131 °C; ^{1}H NMR ($CDCl_3$) δ 0.25 (3H, s), 2.16 (3H, s), 2.63 (3H, s), 3.93 and 4.10 (2H, ABq, J = 13.3 Hz), 7.16–7.27 (7H, m), 7.39–7.45 (2H, m); ^{13}C NMR ($CDCl_3$) δ 4.7 (br), 46.6, 48.3, 67.8, 121.6, 125.1, 126.1, 127.0, 127.1, 130.5, 133.7, 138.5, 147.9 (br), 155.7 (br); ^{11}B NMR ($CDCl_3$) δ 6.8 (half-band width 106 Hz); Anal. Found: C, 80.91; H, 8.55; N, 5.71%. Calcd for $C_{16}H_{20}BN$: C, 81.03; H, 8.50; N, 5.91%.

[2-(Dimethylaminomethyl)phenyl]fluorophenylborane (6c). To a solution of 105 mg (0.41 mmol) of **6a** in 6 mL of acetonitrile was added 89.4 mg (0.70 mmol) of silver fluoride under argon atmosphere. After the mixture was stirred for 4 h at room temperature, the solvent was evaporated. The residue was extracted with chloroform, and insoluble materials were removed by filtration. The evaporation afforded 73 mg (74%) of the practically pure product as colorless amorphous material; mp 75.0–76.5 °C; ^{1}H NMR ($CDCl_3$) δ 2.23 (3H, s), 2.76 (3H, d, J_{HF} = 2.1 Hz), 3.94 and 4.34 (2H, ABq, J = 13.6 Hz), 7.20 (1H, m), 7.21–7.35 (6H, m), 7.47–7.53 (2H, m); ^{13}C NMR ($CDCl_3$) δ 44.7 (d, J_{CF} = 8.1 Hz), 47.5, 67.0, 122.4, 127.4, 127.5, 131.6, 133.1, 133.2, 135.0, 140.2 (Two aromatic signals are missing because of complicated couplings); ^{11}B NMR ($CDCl_3$) δ 12.6 (half-band width 162 Hz); Anal. Found: C, 74.51; H, 7.18; N, 5.72%. Calcd for $C_{15}H_{17}BFN$: C, 74.72; H, 7.11; N, 5.81%.

[2-(Dimethylaminomethyl)phenyl]phenyl(trifluoroacetoxy)borane (6d). To a solution of 118 mg (0.46 mmol) of **6a** in 3 mL of dichloromethane was added 102 mg (0.46 mmol) of silver trifluoroacetate under argon atmosphere. After the mixture was stirred for 1 h at room temperature, the solid was removed by filtration. The filtrate was evaporated, and the residue was recrystallized from hexane–dichloromethane to give 121 mg (79%) of the pure product as colorless crystals; mp 134–136 °C; ^{1}H NMR ($CDCl_3$) δ 2.23 (3H, s), 2.90 (3H, s), 3.96 and 4.48 (2H, ABq, J = 13.5 Hz), 7.20 (1H, m), 7.31–7.44 (7H, m), 7.80 (1H, m); ^{13}C NMR ($CDCl_3$) δ 44.3, 48.2, 67.9, 115.0 (q, J_{CF} = 286.3 Hz), 122.0, 127.3, 127.6, 127.7, 127.8, 132.7, 134.0, 139.7, 140.0 (br), 143.5 (br), 155.8 (q, J_{CF} = 39.6 Hz); ^{11}B NMR ($CDCl_3$) δ 11.3 (half-band width 81 Hz); ^{19}F NMR ($CDCl_3$) δ −72.6; IR (nujol) 1748 cm^{-1} (C=O); Anal. Found: C, 60.57; H, 4.89; N, 4.42%. Calcd for $C_{17}H_{17}BF_3NO_2$: C, 60.93; H, 5.11; N, 4.18%.

[2-(Dimethylaminomethyl)phenyl](pentafluoropropionyloxy)phenylborane (6e). This compound was similarly prepared from **6a** and silver pentafluoropropionate as above. Yield 66%; mp 140–142 °C; ^{1}H NMR ($CDCl_3$) δ 2.22 (3H, s), 2.89 (3H, s), 3.95 and 4.46 (2H, ABq, J = 13.2 Hz), 7.19 (1H, d, J = 7.2 Hz), 7.28–7.32 (5H, m), 7.41 (2H, m), 7.78 (1H, d, J = 7.2 Hz); ^{13}C NMR ($CDCl_3$) δ 44.7, 48.2, 67.8, 105.9 (tq, J_{CF} =

261.1, 38.8 Hz), 118.1 (tq, $J_{CF} = 34.7$, 283.7 Hz), 122.1, 127.3, 127.7, 127.80, 127.83, 132.7, 133.9, 139.4 (br), 139.8, 143.7 (br), 156.5 (t, $J_{CF} = 27.7$ Hz); ^{11}B NMR ($CDCl_3$) δ 8.8 (half-band width 240 Hz); ^{19}F NMR ($CDCl_3$) δ −79.1, −117.6; IR (nujol) 1742 cm^{-1} (C=O); Found: C, 55.89; H, 4.78; N, 3.94%. Calcd for $C_{18}H_{17}BF_5NO_2$: C, 56.13; H, 4.45; N, 3.64%.

Enantiomeric Resolution. The chiral HPLC was carried out with a Daicel Chiralpak AD column (1 cm ϕ × 25 cm). About 2 mg of a racemic sample was injected for each batch. For the resolution of **6e**, the enantiomers were eluted at 21.0 and 27.7 min with the baseline separation (eluent: hexane–2-propanol = 50:1, flow rate 2.0 mL min^{-1}). Easily eluted isomer (+)-**6e**: mp 161–162 °C, $[\alpha]_D^{22}$ +180 (*c* 0.10, acetone), CD (hexane) λ ($\Delta\varepsilon$) 224 (−4.2), 215 (sh, +24). Less easily eluted isomer (−)-**6e**: mp 161–162 °C, $[\alpha]_D^{22}$ −180 (*c* 0.10, acetone), CD (hexane) λ ($\Delta\varepsilon$) 224 (+3.8), 215 (sh, −23). For **6d**, the enantiomers were eluted at 16.2 and 16.6 min with partial separation (eluent: hexane–2-propanol = 1:1, flow rate 1.0 mL min^{-1}). Chiroptical measurements were carried out with partially resolved samples, of which the enantiomeric excess was unknown. The first fraction: $[\alpha]_D^{22}$ +17 (*c* 0.10, acetone), CD (hexane, 4.1×10^{-4} mol L^{-1}) λ (θ/mdeg) 224 (−3.0), 210 (sh, +13.7). The second fraction: $[\alpha]_D^{22}$ −18 (*c* 0.12, acetone), CD (hexane, 4.4×10^{-4} mol L^{-1}) λ (θ/mdeg) 224 (+2.3), 210 (sh, −13.5). Complexes **6b** and **6c** were eluted as single peaks without resolution.

Saturation Transfer Measurement. The measurements were carried out on a JEOL Lambda-500 spectrometer at 500 MHz (^{1}H). The temperature was read from a thermocouple after the calibration with proton chemical shifts of 1,2-ethanediol. About 10 mg of sample was dissolved in ca. 0.7 mL of TCE or nitrobenzene-d_5, and the solution was degassed by bubbling argon gas. The sample was kept at a constant temperature in the range of 120–140 °C throughout the measurement. After the 90° pulse width was determined in an ordinary manner, the effective spin lattice relaxation time (T_{1eff}/s) was measured by the inversion-recovery method. The intensity of one of the Me signals at the lower magnetic field was monitored under the irradiation of the other Me signal. The rate of site exchange (k/s^{-1}) was calculated according to the following equation: $k = [(m/m_0)^{-1} - 1]/T_{1eff}$, where m and m_0 are signal intensities under and without irradiation, respectively. The data for each compound are as follows, where the solvent is TCE unless otherwise mentioned. **6a**: $T_{1eff} = 2.5$ s, $m/m_0 = 0.90$ at 135 °C. **6b**: $T_{1eff} = 2.0$ s, $m/m_0 = 0.40$ at 140 °C. **6c**: $T_{1eff} = 0.36$ s, $m/m_0 = 0.52$ at 120 °C. **6c** (nitrobenzene-d_5): $T_{1eff} = 0.52$ s, $m/m_0 = 0.48$ at 120 °C. **6d**: $T_{1eff} = 0.71$ s, $m/m_0 = 0.92$ at 135 °C. No magnetization transfer ($m/m_0 \approx 1$) was observed for **6e** at 135 °C.

Classical Kinetics. About 1 mg of an enantiopure sample of **6e** was dissolved in 5 mL of heptane. The solution was heated at a constant temperature. The enantiomeric ratio x (= [B]/[A], where A is the starting enantiomer and B is the other enantiomer) was monitored by chiral HPLC at appropriate intervals. The kinetics was analyzed as reversible first-order equilibrium between two enantiomers (A ⇆ B) by the equation of $\ln[(1+x)/(1-x)] = 2kt$, where k is the rate of enantiomerization. The rate constants k/s^{-1} are as follows: $(1.4 \pm 0.2) \times 10^{-5}$ at 73 °C, $(3.1 \pm 0.3) \times 10^{-5}$ at 78 °C, $(6.4 \pm 0.2) \times 10^{-5}$ at 83 °C, $(1.1 \pm 0.2) \times 10^{-4}$ at 88 °C, and $(2.3 \pm 0.5) \times 10^{-4}$ at 93 °C. For **6d**, the measurement was carried out with a partially resolved sample in heptane at 73 °C. The course of isomerization was followed by the angle of ellipticity θ at 215 nm in the CD spectra. The rate constant k was obtained by the least-square fitting of the equation: $\ln(\theta_t/\theta_0) = -2kt$, where θ_0 and θ_t are the ellipticity at time 0 and t, respectively, to give $k = (9.6 \pm 0.3) \times 10^{-5}$ s^{-1}.

X-ray Analysis. Single crystals of **6a**, **6b**, and **6e** were obtained by crystallization from hexane–dichloromethane solutions. The diffraction data were collected on a Rigaku RAXIS-IV imaging plate diffractometer with Mo Kα radiation ($\lambda = 0.71070$ Å) to a maximum 2θ value of 55.1°. The reflection data were corrected for the Lorentz-polarization effects and secondary extinction. The structure was solved by the direct method (SIR 92) and refined by the full-matrix least-squares method by using a teXsan program on a comtec O2 workstation. The non-hydrogen atoms were refined anisotropically. Some hydrogen atoms were refined isotropically, and the rest were included in fixed positions. The additional crystal and analysis data are listed in Table 4. Crystallographic data

Table 4. Crystal Data of Compounds **6a**, **6b**, and **6e**

	6a	**6b**	**6e**
Formula	$C_{15}H_{17}BClN$	$2\cdot C_{16}H_{20}BN$	$C_{18}H_{17}BF_5NO_2$
F. W.	257.57	237.15 × 2	385.14
Crystal size/mm^3	0.3 × 0.3 × 0.5	0.4 × 0.4 × 0.5	0.3 × 0.4 × 0.4
t/°C	−50	−50	−180
Crystal system	monoclinic	orthorhombic	orthorhombic
Space group	$P2_1/n$ (#14)	$Pca2_1$ (#29)	$P2_12_12_1$ (#19)
a/Å	13.694(2)	12.924(1)	7.6462(5)
b/Å	6.595(1)	6.790(1)	14.407(1)
c/Å	16.314(2)	31.292(2)	16.385(1)
β/°	109.17(2)	90	90
V/Å^3	1391.7(4)	2745(1)	1804.9(2)
Z	4	4	4
D_c/g cm^{-3}	1.229	1.147	1.417
μ/cm^{-1}	2.55	0.65	1.25
No. of data	2869	3025	2170
p	0.194	0.140	0.100
$R1$	0.055	0.048	0.085
$wR2$	0.207	0.161	0.138
GOF	1.01	1.02	1.11

for the structures in this paper have been deposited at the Cambridge Crystallographic Data Centre as supplementary publication numbers CCDC 247164 (**6a**), 247165 (**6b**), and 227362 (**6e**).

This work was partly supported by a grant from the Promotion and Mutual Aid Corporation for Private Schools of Japan. The authors thank Messrs. T. Shimasaki and S. Hirano for their assistance of the X-ray analysis, and T. Yamamoto for his technical assistance.

References

A part of this work was preliminary reported as communication. See Ref. 1.

1 S. Toyota, T. Hakamata, N. Nitta, and F. Ito, *Chem. Lett.*, **33**, 206 (2004).

2 Applications of the DMP and related chelating ligands: a) I. Omae, *Coord. Chem. Rev.*, **83**, 137 (1988). b) I. Omae, "Organometallic Intramolecular Coordination Compounds," Elsevier, Amsterdam (1986), p. 35.

3 S. Toyota and M. Ōki, *Bull. Chem. Soc. Jpn.*, **63**, 1168 (1990).

4 S. Toyota and M. Ōki, *Bull. Chem. Soc. Jpn.*, **64**, 1554 (1991).

5 a) S. Toyota, T. Futawaka, M. Asakura, H. Ikeda, and M. Ōki, *Organometallics*, **17**, 4155 (1998). b) S. Toyota, T. Futawaka, H. Ikeda, and M. Ōki, *J. Chem. Soc., Chem. Commun.*, **1995**, 2499.

6 a) S. Toyota and M. Ōki, *Bull. Chem. Soc. Jpn.*, **65**, 2215 (1992). b) S. Toyota, M. Asakura, T. Futawaka, and M. Ōki, *Bull. Chem. Soc. Jpn.*, **72**, 1879 (1999).

7 S. Toyota and M. Ōki, *Bull. Chem. Soc. Jpn.*, **65**, 1832 (1992).

8 T. Murafuji, K. Kurotobi, N. Nakamura, and Y. Sugihara, *Curr. Org. Chem.*, **6**, 1469 (2002), and references therein.

9 For example, a dynamic NMR study of configurational stability in cyclic borates: S. Green, A. Nelson, S. Warriner, and B. Whittaker, *J. Chem. Soc., Perkin Trans. 1*, **2000**, 4403.

10 a) D. J. Owen, D. VenDerveer, and G. B. Schuster, *J. Am. Chem. Soc.*, **120**, 1705 (1998). b) D. J. Owen and G. B. Schuster, *J. Am. Chem. Soc.*, **118**, 259 (1996).

11 a) E. Vedejs, R. W. Chapman, M. Müller, and D. R. Powell, *J. Am. Chem. Soc.*, **122**, 3047 (2000). b) E. Vedejs, S. C. Fields, R. Hayashi, S. R. Hitchcock, D. R. Powell, and M. R. Schrimpf, *J. Am. Chem. Soc.*, **121**, 2460 (1999).

12 A. R. Rico, M. Tlahuextl, A. Flores-Parra, and R. Contreras, *J. Organomet. Chem.*, **581**, 122 (1999).

13 O. N. Shevtsova and A. M. Yurkevich, *Zh. Obshch. Khim.*, **46**, 348 (1976).

14 a) H. I. Beltran, L. S. Zamudio-Rivera, T. Mancilla, R. Santillan, and N. Farfan, *J. Organomet. Chem.*, **657**, 194 (2002). b) T. Mancilla and R. Contreras, *J. Organomet. Chem.*, **321**, 191 (1987).

15 C. S. Shiner, C. M. Garner, and R. C. Haltiwanger, *J. Am. Chem. Soc.*, **107**, 7167 (1985).

16 P. Vedrenne, V. Le Guen, L. Toupet, T. Le Gall, and C. Mioskowski, *J. Am. Chem. Soc.*, **121**, 1090 (1999).

17 T. Imamoto and H. Morishita, *J. Am. Chem. Soc.*, **122**, 6329 (2000).

18 L. Charoy, A. Valleix, L. Toupet, T. Le Gall, P. P. van Chuong, and C. Mioskowski, *Chem. Commun.*, **2000**, 2275.

19 Substitution of phenyl groups at boron atoms tends to strengthen the B–N coordination bond compared with alkyl groups in the (DMP)borane system. For instance, the tight coordination bond in {[1-(dimethylamino)ethyl]phenyl}diphenylborane was reported: L. Horner, U. Kaps, and G. Simons, *J. Organomet. Chem.*, **287**, 1 (1985).

20 H. Nöth and B. Wrackmeyer, "Nuclear Magnetic Resonance Spectroscopy of Boron Compounds," Sprinter Verlag, Berlin (1978).

21 R. G. Kidd, "NMR of Newly Accessible Nuclei," ed by P. Laszlo, Academic Press, New York (1983), Vol. 2, Chap. 3.

22 ^{11}B NMR data of similar borane–amine complexes taken from Ref. 20. $Me_3N{\rightarrow}BEt_2Cl$ (δ 11.7), $Me_3N{\rightarrow}BEt_2F$ (δ 9.5), $Me_3N{\rightarrow}BEt_3$ (δ 4.3), (*N–B*)-$Bu_2B(CH_2)_3NEt_2$ (δ 7.0), (*N–B*)-$PhB[(CH_2)_3]_2NEt$ (δ 9.4), (*N–B*)-$Bu(AcO)B(CH_2)_3NMe_2$ (δ 8.3), and (*N–B*)-$Et_2BOCOCH_2NHMe$ (δ 10.0).

23 The Cambridge Crystallographic Database (CSD ver. 5.25) analysis was carried out for the substructures of $C_3N{\rightarrow}BC_2X$ (X = C, O, or Cl). A total of 15 structures were found except compounds with strongly electron-withdrawing groups or sterically strained structures. The ranges of the B–N bond distances are 1.68–1.76 Å (for 7 structures of X = C), 1.67–1.74 Å (for 7 structures of X = O), and 1.69 Å (for 1 structure of X = Cl).

24 H. Höpfl, *J. Organomet. Chem.*, **581**, 129 (1999).

25 H.-B. Tong, X.-H. Wei, S.-P. Huang, J.-F. Lia, and D.-S. Liua, *Acta Crystallogr., Sect. E*, **58**, 1389 (2002).

26 a) S. Forsén and R. A. Hoffman, *J. Chem. Phys.*, **39**, 2892 (1963). b) R. A. Hoffman, B. Gestblom, and S. Forsén, *J. Chem. Phys.*, **39**, 486 (1963). c) S. Forsén and R. A. Hoffman, *Acta Chem. Scand.*, **17**, 1787 (1963).

27 Reliability of kinetic data determined by the ST method compared with those determined by other kinetic methods, see: M. Nakamura, H. Kihara, N. Nakamura, and M. Ōki, *Org. Magn. Reson.*, **12**, 702 (1979).

28 Enantiomerization means the conversion of one enantiomer into the other, and racemization means the conversion of an enaniopure or enantioenriched material into a racemate. Therefore, the rate of racemization (k_{rac}) is double of the rate of enantiomerization, $k_{rac} = 2k_{ena}$.

29 a) C. H. Bushweller, "Acyclic Organonitrogen Stereodynamics," ed by J. B. Lambert and Y. Takeuchi, VCH, New York (1992), Chap. 1. b) J. B. Lambert, *Top. Stereochem.*, **6**, 19 (1971).

30 a) P. Finocchiaro, D. Gust, and K. Mislow, *J. Am. Chem. Soc.*, **95**, 7029 (1973). b) B. Meissner and H. A. Staab, *Justus Liebigs Ann. Chem.*, **753**, 92 (1971). c) J. F. Blount, P. Finocchiaro, D. Gust, and K. Mislow, *J. Am. Chem. Soc.*, **95**, 7019 (1973).

31 J. D. Odom, "Comprehensive Organometallic Chemistry," ed by G. Wilkinson, F. G. A. Stone, and E. W. Abel, Pergamon Press, Oxford (1982), Vol. 1, Chap. 5.1.

32 The entropies of activation ($\Delta S^{\neq}$) of the dissociation of B–N coordination bond in **1** and **2** are 56 and 64 $J\,mol^{-1}\,K^{-1}$, respectively. See Refs. 3 and 4.

33 a) M. K. Murphy and J. L. Beauchamp, *Inorg. Chem.*, **16**, 2437 (1977). b) V. Jones, G. Frenking, and M. T. Reetz, *J. Am. Chem. Soc.*, **116**, 8741 (1994).

34 "Ionisation Constants of Organic Acids in Aqueous Solutions," ed by E. P. Serjeant and B. Dempsey, Pergamon Press, Oxford (1979).